Waste Gasification in a Melting Updraft Moving Bed Reactor: Preliminary Analysis on Oxidation and Melting Zone

Alessia Borgogna[a,*], Annarita Salladini[b], Maria Cristina Annesini[a], Gaetano Iaquaniello[b]

[a] Dip. Ingegneria Chimica Materiali e Ambiente, Sapienza Università di Roma, Via Eudossiana 18, 00184 Roma (Italy)
[b] NextChem s.r.l., Via di Vannina 88, 00156, Rome (Italy)
 alessia.borgogna@uniroma1.it

Waste conversion into valuable chemical products seems to be a good overcoming strategy both for the fossil fuel resources employment and for the current inefficient waste management. The main step related to the production of chemical from waste is its thermochemical conversion via gasification process. Taking into account the variable composition of waste and its high ash amount, among others, the high temperature melting gasifier is the most suitable system for ensuring the required flexibility. Indeed, besides syngas production, this system allows the melting of waste ash fraction in order to produce a vitrified and inert granular material. A simplified transient one-dimensional model of the oxidation zone including melting phenomenon could help in the understanding of process behavior.

1. Introduction

During the last century, gasification processes have been extensively investigated through experimental and theoretical studies, due to their relevance in different industrial fields. While coal has been always considered as the primary feedstock of these thermal conversion processes, in the recent years, the increasing awareness regarding sustainability triggers researches in the field of thermal conversion of renewable resources, as biomass and waste. In particular, waste thermal conversion does not only represent an alternative to the conventional waste treatments, but it can be exploited as a new possible way to produce energy and chemicals. As example, the waste to methanol process has been demonstrated being feasible both from a technical and economic point of views (Iaquaniello et al., 2017; Salladini et al. 2018 a). The core of this kind of process is the high temperature melting gasifier, a scheme is depicted in Fig.1-a. The bottom section works like a moving bed gasifier where, at the same time, syngas is produced from the combustible fraction of waste and a stable granular material is obtained from the inert one. The upper section, instead, provides the stabilization of syngas ensuring the production of a syngas lack of harmful and troublesome products. As a result, this specific system provides performances and flexibility required for the conversion of a complex material such as waste; indeed, gasification of waste must face several criticisms, one of these is the high ash content of waste. To overcome to this issue, the applied oxidant agent is oxygen, rather than air; that allows to reach higher temperature (>1600 °C) ensuring the melting of the ash fraction, which flows out the reactor as a slag and then is cooled and collected as vitrified material. This feature mostly differentiates this reactor from the more traditional ones, in which, instead, ash melting is expressly prevented. As matter of fact, if the system is not just design for that, melted ash could cause serious technical complications. Mathematical modelling of waste gasification is a powerful tool for the gasifier design and simulation of its behavior in different operating conditions, for example also accounting for waste composition variability. A first modelling approach should be a thermodynamic model. In particular, thermodynamic model of the high temperature melting waste gasification has been developed in order to understand the influence of operating condition and waste composition variability on syngas production (Salladini et al., 2018 b). Indeed, waste presents a variable composition able to affect gasification products: both the syngas and the inert slag. Waste composition can be characterized by its LHV and three main pseudo-components which are the combustible

(50-80%), the moisture (10-25%) and the ash fractions (10-25%). Thus, syngas yield is mostly related to the combustible fraction, instead syngas composition depends mainly on LHV and combustible fraction composition; finally, slag quantity directly corresponds to the ash fraction amount. However, obviously, the thermodynamic approach does not account for the process dynamics, which requires a more detailed model including kinetics and transport aspects. Different efforts have been made towards the development of detailed mathematical model of gasification/combustion (see for example Pierucci and Ranzi, 2008; Hobbs et al., 1992). For fixed/moving bed, one-dimensional kinetic are widely investigated and used for different applications (Di Blasi, 2004; Hla, 2004). In these models, the fuel bed is usually ideally schematized in stratified reaction zones, wherein one type of reaction predominantly occurs: from the top to the bottom, drying, pyrolysis, partial oxidation and oxidation and melting zones (see. Fig. 1-b) are considered. The long-term purpose is to derive a model for the melting updraft moving bed gasifier above mentioned (see Fig. 1) where solid waste, Refuse Derived Fuel (RDF) or plastic waste, and oxygen (gasification agent) are fed counter-currently. In this work, as preliminary approach, we focus only on the modeling of partial oxidation and oxidation and melting zones, including the thermal aspect related to the melting of inert fraction. The study here presented has the aims of figuring out a way to include melting phenomenon into established moving bed mathematical model.
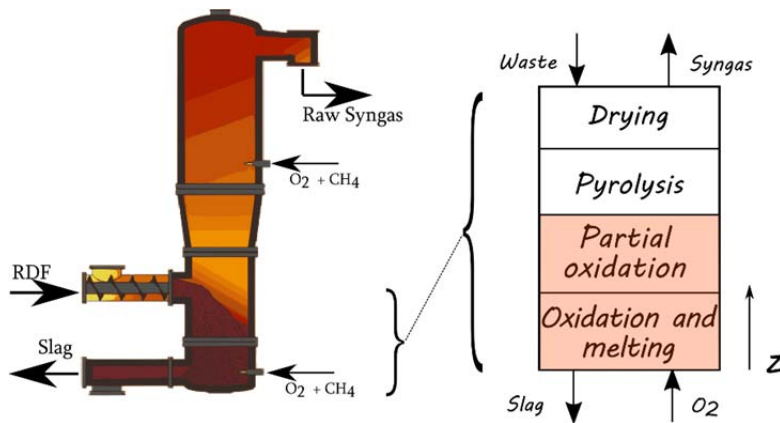

Figure 1. Sketch of a high temperature melting gasifier. A schema of moving melting bed, with the main reaction zones is reported on the right panel.

2. Problem description and model approach

In order to model the oxidation/melting and partial oxidation zones, two components (char and unreactive ash, representing fixed carbon and ash fractions of waste) and six species (H_2, CO, CO_2, H_2O, N_2, CH_4) are considered for the solid and gas phases, respectively.

Both homogeneous (in the gas phase) and heterogeneous (gas-solid) reactions are considered (see Table 1).

As reported in Figure1, the gasifying agent, which enter at z=0, flows upwards counter-currently to the descending solid, just coming from the pyrolysis zone. In the modeling, this solid phase is assumed to be represented by spherical monodispersed particles whose dimension decreases due to the heterogeneous reactions. A dynamic one-dimensional model, based on the mass and heat balance equations described in the next paragraph, is implemented in Comsol Multiphysics environment, with the introduction of customized partial derivative equations. The domain mesh has been built considering the higher gradient existing in the entering zone where highly exothermic reactions take place. Thus, a variable Δz, increasing along the z-direction, has been chosen; a final mesh of 761 elements is achieved.

Model equations

In the modeling, gas and solid phases are considered as interpenetrating continua, i.e. each finite discrete element is assumed to be composed of both phases according to the respective volume fractions, hereafter referred as ε_g and $\varepsilon_s = 1 - \varepsilon_g$. Mass and heat exchange between phases are considered.

As for the gas phase, the model is built up with the continuity equation (1), the enthalpy balance (2) and mass balance (3) for each *i-th* gas species.

$$\varepsilon_g \frac{\partial \rho_g}{\partial t} + \varepsilon_g \frac{\partial \rho_g v_g}{\partial z} = M_{s \rightarrow g} \tag{1}$$

$$\varepsilon_g \frac{\partial \rho_g cp_g T_g}{\partial t} + \varepsilon_g \frac{\partial \rho_g v_g cp_g T_g}{\partial z} = \frac{\partial}{\partial z}\left(\varepsilon_g \frac{\partial \lambda_g^* T_g}{\partial z}\right) + Q_{s \to g} - Q_{g \to w} + \sum_{j=1}^{r_{hom}} (-\Delta H_j r_j) \tag{2}$$

$$\varepsilon_g \frac{\partial \rho_g w_i}{\partial t} + \varepsilon_g \frac{\partial \rho_g v_g w_i}{\partial z} = \frac{\partial}{\partial z}\left(\varepsilon_g \frac{\partial D_i \rho_g w_i}{\partial z}\right) + M_i \sum_{j=1}^{r_{hom}} v_{ij} r_j + \frac{M_i}{M_c} \sum_{k=1}^{r_{het}} v_{ik} R_k \tag{3}$$

where $M_{s \to g}$ is the mass flow between the solid and the gas phase, $Q_{s \to g}$ and $Q_{g,s \to w}$ are the heat flow exchanged between the solid and the gas phase and between the gas and solid phases and the reactor wall respectively. Momentum balance is not fully resolved. However, gas phase pressure, P_g, density, ρ_g, and velocity, v_g, are linked and assessed considering the Ergun equation (4) and ideal gas law (5).

$$\frac{\partial P_g}{\partial t} = -A v_g - B v_g |v_g|, \qquad A = \frac{150 \mu_g (1 - \varepsilon_g)^2}{\varepsilon_g{}^3 d_p{}^2} \qquad B = \frac{150 \rho_g (1 - \varepsilon_g)}{\varepsilon_g{}^3 d_p} \tag{4}$$

$$\rho_g = \frac{P_g R T_g}{M_g} \tag{5}$$

As for the solid phase, the continuity equation (6) and mass balance for char and ash (7-8) are considered:

$$\boldsymbol{\varepsilon_s \frac{\partial \rho_s}{\partial t} + \varepsilon_s \frac{\partial \rho_s u_s}{\partial z} = -M_{s \to g}} \tag{6}$$

$$\boldsymbol{\varepsilon_s \frac{\partial \rho_c \phi_c}{\partial t} + \varepsilon_s \frac{\partial \rho_c u_s \phi_c}{\partial z} = -M_{s \to g}} \tag{7}$$

$$\boldsymbol{\varepsilon_s \frac{\partial \rho_a \phi_a}{\partial t} + \varepsilon_s \frac{\partial \rho_a u_s \phi_a}{\partial z} = 0} \tag{8}$$

The enthalpy balance is written as

$$\boldsymbol{\varepsilon_s \frac{\partial \rho_s cp_s T_s}{\partial t} + \varepsilon_s \frac{\partial \rho_s v_s cp_s T_s}{\partial z} = \frac{\partial}{\partial z}\left(\varepsilon_s \frac{\partial \lambda_s^* T_s}{\partial z}\right) - Q_{s \to g} - Q_{s \to w} + \sum_{k=1}^{r_{het}} (-\Delta H_k R_k)} \tag{9}$$

where the heat of reaction is explicitly accounted for. Obviously, the solid heat capacity results from char and ash heat capacity. As mentioned in the introduction, differently from the other conventional systems, ash melting occurs at the bottom of a melting furnace; in order to account for the large heat amount required for this phenomenon, in the heat balance, a correct form of the ash heat capacity is introduced (Samara et al., 2012). Taking into account data from literature (Mills, 1986; Holubcik, 2015) it is assumed that melting occurs in a temperature range between T_m and $T_m + \Delta T_m$ and a piecewise function has been introduced for the ash heat capacity

$$cp_a [kJ (kgK)^{-1}] = \begin{cases} cp_{a,s} = 0.99 + 2.98 \cdot 10^{-4} T_s + +2.11 \cdot 10^{-6} T_s{}^{-2} & T \leq T_m \\ \dfrac{cp_{a,s}(T_m) + cp_{a,l}}{2} + \dfrac{\Lambda_m}{\Delta T_m} & T_m < T \leq T_m + \Delta T_m \\ cp_{a,l} = 1.48 & T \geq T_m + \Delta T_m \end{cases}$$

A value of 600 kJ/kg is used for the latent heat of ash melting Λ_m, while T_m and ΔT_m are set 1100°C and 100°C respectively (Holubcik, 2015).

Again, a momentum balance equation has not been considered, whereas solid velocity profile, u_s, is resolved only considering bed shrinking which occurs due to the decrease in particle size. In details, the solid velocity is driven by solid consumption ($M_{s \to g}$) and thus it is obtained solving the continuity equation (6) coupled with the conservation of particle number per element $\dot{N}_p$:

$$\boldsymbol{\frac{\partial}{\partial t}\left(\frac{\dot{N}_p}{\varepsilon_s}\right) + \frac{\partial}{\partial z}\left(\frac{\dot{N}_p u_s}{\varepsilon_s}\right) = \frac{\partial}{\partial t}\left(\frac{1}{V_p}\right) + \frac{\partial}{\partial z}\left(\frac{u_s}{V_p}\right) = 0} \tag{10}$$

Indeed, equation (10) is derived assuming that generation, agglomeration or reduction of particle number per element do not occur and that solid volume fraction (ε_s) is fixed (Cooper and Hallet, 2000). Mass flow exchange between solid and gas is given by the net gas production rate due to the heterogeneous reactions $M_{s \to g} = \sum R_k$, while the heat flows can be expressed in terms of a suitable heat transfer coefficient and the

corresponding temperature difference. A list of the relationships to evaluate the model parameters is reported in Table 2, while the physical properties are summarized in Table 3. Reaction kinetics and kinetic coefficients are taken from literature data (Di Blasi, 2004; Hla, 2004): as for heterogenous reactions, the effective reaction rate, R_k, is obtained combining chemical and diffusional kinetics, with a mass transfer coefficient through the gas film expressed as a function of the gas flow rate; a maximum value (k_m^l set to 0.2 m s^{-1}) of the mass transfer coefficient is introduced in order to avoid unrealistic temperature which may arise mostly for low Re number (Di Blasi, 2004). The heat coefficient transfer between phases and wall $h_{g,s \to w}$ has been estimated (2.5 kW/mK) in order to achieve a good agreement between simulated and expected (from plant experiences) temperatures.

Table 1. Reactions.

Homogeneous	
r1	$CH_4 + 1.5\ O_2 \rightarrow CO + 2\ H_2O$
r2	$CO + 0.5\ O_2 \rightarrow CO_2$
r3	$H_2 + 0.5\ O_2 \rightarrow H_2O$
r4	$CO + H_2O \leftrightarrow CO_2 + H_2$
Heterogenous	
R1	$C + \gamma\ O_2 \rightarrow (2 - 2\gamma)\ CO + (2\gamma - 1)\ CO_2$
R2	$C + CO_2 \rightarrow 2\ CO$
R3	$C + H_2O \rightarrow CO + H_2$
R4	$C + 2\ H_2 \rightarrow CH_4$

Table 2. Relationships used for model parameter evaluation.

A_p	$6 \dfrac{(1-\varepsilon_g)}{d_p}$	
$h_{s \to g}$	$2.06 \dfrac{cp_g \rho_g v_g}{Re^{0.575} Sc^{2/3}}$	
R_k	$\dfrac{M_c}{\nu_k M_k} \dfrac{A_p \rho_g w_k}{\left(\frac{1}{k_m}+\frac{1}{k_k}\right)}$	$\phi_c > 0$
k_m	$2.06 \dfrac{v_g}{Re^{0.575} Sc^{2/3}}$	$k_m < k_m^l$

Table 3. Proprieties of gas and solid.

Gas heat capacity [kJ (kgK)$^{-1}$]	cp_g	$9.4 \cdot 10^2 + 1.67 \cdot 10^{-1}\ T_g + 6.51 \cdot 10^{-5}\ T_g^2$
Gas viscosity [Pa s]	μ_g	$1.97 \cdot 10^{-5}\ (T_g/300)^{2/3}$
Ash heat capacity [kJ (kgK)$^{-1}$]	cp_a	See in text
Ash density [kg m^{-3}]	ρ_a	1800
Char heat capacity [kJ (kgK)$^{-1}$]	cp_c	$1.39 \cdot 10^3 + 3.6 \cdot 10^{-1}\ T_s$
Char density [kg m^{-3}]	ρ_c	800
Gas thermal conductivity [W (mK)$^{-1}$]	$\lambda_g^* = \varepsilon_g \lambda_g$	$\varepsilon_g (4.77 \cdot 10^{-4}\ T_g^{0.717})$
Solid thermal conductivity [W (mK)$^{-1}$]	$\lambda_s^* = f(\lambda_s)$	see reference Di Blasi, 2004; $\lambda_s = 0.13 + 3 \cdot 10^{-4}\ T_s$
Species diffusion coefficients [m^2 s^{-1}]	D_i	$10^{-5}\ (T_g/273.15)^{2/3}$

3. Results and discussion

Boundary and initial conditions

The proposed model has been applied to simulate the behavior of oxidation and melting zone of a full-scale gasifier with a diameter of 2.6 m. The height of the simulated bed zones is set equal to 0.25 m: preliminary model results show that the reactions go to completion within this area. Fresh oxygen plus a little amount (3%wt) of CH_4 as auxiliary fuel with a mass flow rate of 2 ton h^{-1} enters from the burners located at the bottom of the gasifier. In the model we directly consider the introduction of the gas mixture obtained from the CH_4 oxidation ($w_{O2}=0.804$; $w_{CO2}=0.081$; $w_{H2O}=0.066$; $w_{N2}=0.049$; $w_{CO}=0$; $w_{CH4}=0$) at the adiabatic combustion temperature ($T_g^0 \sim 1150$ °C). The resulting inlet gas velocity is then equal to 0.78 m s^{-1}. As for the solid phase, a waste flow rate 7 ton h-1 is fed to the gasifier with a fixed carbon and ash content equal to 0.045 and 0.15, respectively. Only char and ash are assumed to enter in the gasification zone with a carbon volume fraction

ϕ_c^0=0.403 and a solid velocity u_s^0= 1.3·10-4 m s^{-1}. Assuming that in the drying and pyrolysis shrinking does not occur (Di Blasi, 2004), initial particle size dp^0 should be the same of the particle entering at the top of the reactor, we here consider a value of 25 mm. To ensure ignition, a section of solid bed must be set at an initial temperature near to 1000 °C, thus the initial profiles of solid and gas temperatures are chosen as decreasing functions along reaction height, starting from 1150 °C and 970 °C, respectively, and both reaching, for z=0.25 m, the boundary temperature value of solid phase T_s^0. In the left panel of Figure 2 are shown these profiles in the case T_s^0=400 °C. The inlet temperature T_s^0 is difficult to be a priori estimated, for that, we perform a sensitive analysis in order to point out the influence of this variable. As can be gathered from Figure2-b, the influence is not so significant as regards the of T_g and T_s profiles, on the other hand it is considerable on the gas composition, in detail the higher T_s^0 is higher, the higher the ratio between CO to CO_2 produced. In the forthcomings results T_s^0 has been considered equal to 400 °C, just as base case value. Indeed, in future development wherein all reactor zones are modeled, this value will directly derive from the match of lower and upper section heat balances.
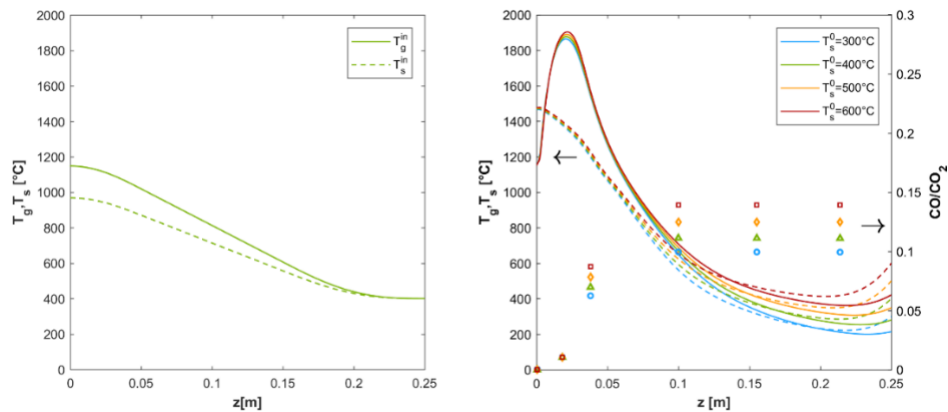

Figure 2. In the left panel (a) T_s and T_g initial condition profiles for T_s^0=400°C; in the right panel (b) T_s, T_g and ratio CO/CO_2 profiles (t=200s) are displayed for different solid temperature boundary condition (T_s^0).

In Figure 3 solid and gas velocity, the solid volume fraction and gas composition profiles are depicted for the base case at t=200s. As it can be seen from the picture, at this time the complete solid consumption has almost just been reached, so as that the oxidation zone is completely settled. In the selected conditions (for which carbon is all converted before that the solid outflows) we then assist to the dynamic translation of reaction front (Figure 4): the oxidation zone moves along the reactor height preserving its width almost equal (from 0.0336 m at t=200s to 0.0344 m at t=500s), instead, T_g and T_s peaks slightly decrease, of about 20°C and 30°C, respectively. This behavior is related to: -the examined conditions which ensure no carbon fraction in the solid output; -the simplifying assumption according to which the solid velocity is supposed to be driven only by mass consumption; -finally, the neglect of fluid dynamic effects associated with melting of ash fraction.
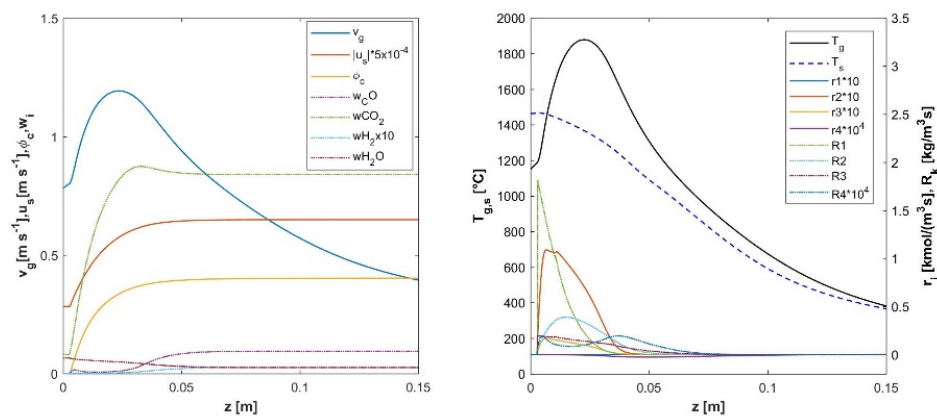

Figure 3. Main variable profile along a section of reaction (0 < z < 0.15 m) with condition of case base mentioned in the text for t= 200 s.
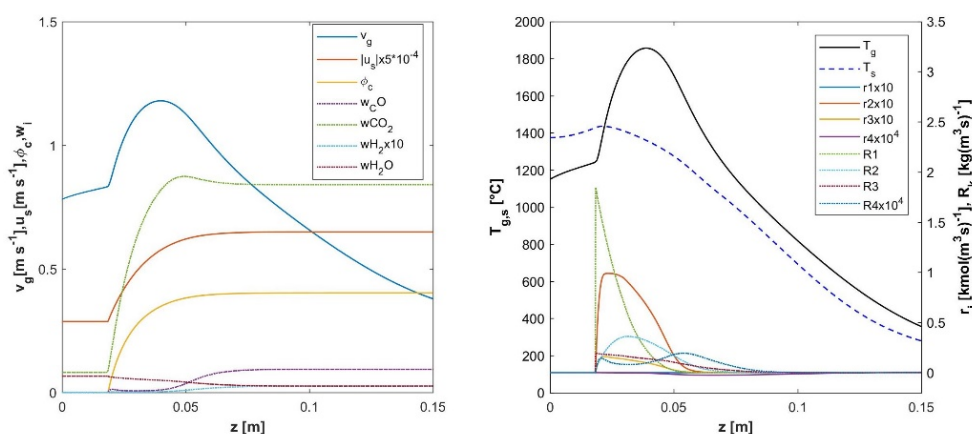
Figure 4. Main variable profile along a section of reaction (0 < z < 0.15 m) with condition of case base mentioned in the text for t= 500 s.

4. Conclusions

This work describes a model aiming at reproducing the behavior of the bottom section of a high temperature melting gasifier; in detail, partial oxidation and oxidation and melting zones have been considered, including the distinctive ash fraction melting occurrence. Thermal aspects related to ash fraction melting have been introduced into the transient model by means of a piecewise function which represents the ash heat capacity dependence on temperature accounting for latent heat required for melting. Then, the system described represents merely a part of the model, which is still a working in progress item, indeed, steps towards modelling all reactor zones and improving the melting phenomenon description are to be made.

References

Cooper, J. and Hallett, W.L.H., 2000. A numerical model for packed-bed combustion of char particles. Chemical Engineering Science, 55(20), pp.4451-4460.

Di Blasi, C., 2004. Modeling wood gasification in a countercurrent fixed-bed reactor. AIChE Journal, 50(9), pp.2306-2319.

Hla, S.S., 2004. A theoretical and experimental study on a stratified downdraft biomass gasifier (Doctoral dissertation, PhD thesis, University of Melbourne).

Hobbs, M.L., Radulovic, P.T. and Smoot, L.D., 1992. Modeling fixed-bed coal gasifiers. AIChE Journal, 38(5), pp.681-702.

Holubcik, M., Jandacka, J. and Malcho, M., 2015. Ash melting temperature prediction from chemical composition of biomass ash. The holistic approach to environment, 5(3), pp.119-125.

Iaquaniello, G., Centi, G., Salladini, A., Palo, E., Perathoner, S. and Spadaccini, L., 2017. Waste-to-methanol: Process and economics assessment. Bioresource technology, 243, pp.611-619.

Mills, K.C., 1986. Estimation of physicochemical properties of coal slags and ashes. American Chemical Soc., 301, pp.195-214.

Pierucci, S. and Ranzi, E., 2008. A general mathematical model for a moving bed gasifier. In Computer Aided Chemical Engineering (Vol. 25, pp. 901-906). Elsevier.

Salladini, A., Agostini, E., Borgogna, A., Spadacini, L., Annesini, M.C. and Iaquaniello, G., 2018 a. Analysis on High Temperature Gasification for Conversion of RDF into Bio-Methanol. In Gasification for Low-grade Feedstock. IntechOpen.

Salladini, A., Borgogna, A., Spadacini, L., Pitrelli, A., Annesini, M. and Iaquaniello, G., 2018 b. Methanol production from Refuse Derived Fuel: A preliminary analysis on the influence of the RDF composition on process yield.

Samara, F., Groulx, D. and Biwole, P.H., 2012, November. Natural convection driven melting of phase change material: comparison of two methods. In Excerpt from the Proceeding of the COMSOL Conference.